



HAL
open science

An inovative optical viscometer using a resonant surface signal

Jordan Gastebois, Hervé Lhermite, Hervé Cormerais, Arnaud Saint-Jalmes,
Véronique Vié, Lucas Garnier, Bruno Bêche

► **To cite this version:**

Jordan Gastebois, Hervé Lhermite, Hervé Cormerais, Arnaud Saint-Jalmes, Véronique Vié, et al.. An inovative optical viscometer using a resonant surface signal. Proceedings of SPIE, the International Society for Optical Engineering, 2023, Optical Metrology, 12622-47, pp.1-9. 10.1117/12.2672418 . hal-04156228

HAL Id: hal-04156228

<https://hal.science/hal-04156228v1>

Submitted on 7 Jul 2023

HAL is a multi-disciplinary open access archive for the deposit and dissemination of scientific research documents, whether they are published or not. The documents may come from teaching and research institutions in France or abroad, or from public or private research centers.

L'archive ouverte pluridisciplinaire **HAL**, est destinée au dépôt et à la diffusion de documents scientifiques de niveau recherche, publiés ou non, émanant des établissements d'enseignement et de recherche français ou étrangers, des laboratoires publics ou privés.

An inovative optical viscometer using a resonant surface signal

J. Gastebois^a, H. Lhermite^a, H. Cormerais^{a,c}, A. St Jalmes^b, V. Vié^b,
L. Garnier^a, and B. Bêche^a

^aUniv Rennes, CNRS, Institut IETR - UMR 6164, F-35000 Rennes, France

^bUniv Rennes, CNRS, Institut IPR - UMR 6251, F-35000 Rennes, France

^cCentrale/Supelec, Campus de Rennes, F-35510 Cesson-Sévigné, France

ABSTRACT

The understanding and analyzing of solid particle behavior in a liquid is a challenge in numerous fields and engineering industry as the petroleum or the cosmetic one. It is indeed essential to know the behavior of soft matter process to avoid problems and ensures the product quality. This study presents the viscosimeter development working on a resonant optical signal principle by measuring the Free Spectral Range (FSR) parameter of a resonant optical mode during nanoparticles (NPs) sedimentation in a liquid which consists of a water/glycerol mixture. The photonic structure is composed of racetracks micro-resonators made of a UV210 polymer fabricated by deep-UV photolithography developed on an oxydated silicon layer to get a Si/SiO_2 bi-layer. The chip is then integrated in an optical bench to track the evolution of the FSR during the complet sedimentation process. The resonant signal analyse established by an adapted signal processing of silica nanoparticles sedimentation in different water/glycerol concentrations allows us to determine stages and velocity rate of the sedimentation process to finally access to their viscosity. At the same time, measures are performed on a commercial mechanical rheometer so as to compare the dynamic evolution of their viscosity and their associated FSR. The plot of those data versus the glycerol concentration in water obviously shows a possible mathematical transformation between viscosity and FSR slope. There is therefore a good agreement between mechanical and resonant optical measures if we consider the dynamic evolution of both curves ; so this work proves the feasibility of an optical viscosimeter based on resonant signal.

Keywords: Integrated photonics and resonators, optical characterizations, viscosity and sedimentation, soft matter, surface resonant signal processing, rheology.

1. INTRODUCTION

Understanding the soft matter behavior is crucial in various fields to ensure product quality and stability.¹ In galenic pharmacology, knowing how active substances behave in colloidal suspensions is important. One specific aspect of soft matter behavior, solid particle sedimentation in liquids, is vital in medicine and the petroleum industry. The speed rate of red blood cells is essential for medical diagnostics, while product quality monitoring is critical for petroleum products.^{2,3}

Optical cavities or micro-resonators (MRs) are have been widely used and integrated into photonic devices for diverse applications and research purposes.^{4,5} They are commonly employed as sensors for chemical detection and biological applications.⁶ Additionally, MRs have recently found application in studying dynamic soft matter processes such as phase transitions⁷ and the evaporation of sessile water droplets.⁸ The present study aims to approach the viscosity of a water/glycerol mixture during a sedimentation process using optical resonant signals. The dispersion equation, derived from the resolution of Maxwell's equations, demonstrates the existence of a mode propagating in a waveguide in both the core (oscillatory solution) and the cladding (evanescent solution).^{9,10} This property is particularly relevant for sensing applications as the surrounding environment interacts

Further author information:

J. Gastebois : E-mail: jordan.gastebois@univ-rennes.fr

B. Bêche: E-mail: bruno.beche@univ-rennes.fr, <https://www.ietr.fr/bruno-beche>

with the evanescent wave in the cladding and therethore altering the optical mode propagation in the waveguide. The evanescent portion of the light serves as a tunable light probe for detecting changes and variations in the environment.¹¹ In this paper, the change is determined by monitoring the evolution of the Free Spectral Range (FSR) during a sedimentation process. In the resonator, a wave in phase coherence after completing one round can circulate and it is described by $P.n_{eff}^{group} = m.\lambda_{res,m}$ with P the perimeter resonator, m an integer, n_{eff}^{group} the effective group index and $\lambda_{res,m}$ the m^{th} resonant wavelength. The Free Spectral Range (FSR), also known as the pseudo period, is defined as the difference between two consecutive resonant wavelengths. It is directly related to the effective group index n_{eff}^{group} , which is related to the mode propagation constant $\beta = k_0 n_{eff}^{group}$, by $FSR = \frac{\lambda_0^2}{P.n_{eff}^{group}}$, with λ_0 the central wavelength of the source. In order to monitor the pseudo-period, racetrack micro-resonators (MRs) are fabricated using a UV210 polymer and shaped through deep UV lithography. The photonic device is then integrated on an experimental setup wherein the resonances are excited using a broadband laser, and the output is connected to an Optical Spectrum Analyzer. This setup enables the collection of signals throughout the entire sedimentation process.

A tank containing the mixture is positioned above the chip surface, creating a *UV210/Mixture_{water/glycerol}* structure. The introduction of a solution containing silica nanoparticles (NPs) leads to a gradual modification of the structure upper cladding made by such effective granular medium and therefore a change in the effective group index. Optical resonance measurements are then compared to mechanical measurements performed with a commercial rheometer. By plotting and analyzing the mechanical and optical data against the glycerol concentration, it is possible to draw conclusions regarding the development of an optical viscometer.

2. MATERIAL AND EXPERIMENTAL SET-UP

2.1 Material and process

The optical cavities are composed of racetrack MRs coupled to a taper¹² access waveguide, with a fixed gap of $g = 400$ nm between the taper and MRs. Designs are made by software and parameters such as R (curvature radius), L_c (coupling length), and w (access waveguide width) are selected to achieve optimal spectral characteristics at dimensions of 5-5-3 μm respectively. To enhance measurement precision and obtain deeper resonant peaks, four MRs are employed. Increasing the number of resonators also extend the coverage to a larger surface area, enabling spatial averaging of the measurements.¹³ The Figure 1 shows the geometrical elements of the so called structure.

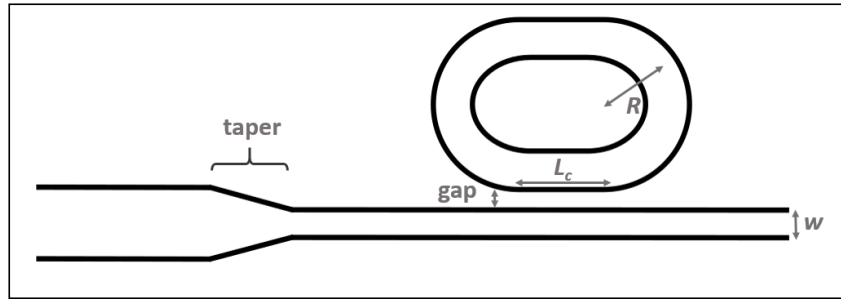


Figure 1. Schematic representation of the architecture of the resonant circuits used as sensors. A racetrack-shaped micro-resonator is coupled to an access waveguide and a taper structure is present at the beginning of the latter in order to facilitate the optical injection.

The waveguide cores are made of a UV210 polymer positive resine, while the lower cladding is composed of a thermal silica layer formed by the wet oxydation method on a 3-inches silicon wafer. The wafer is first clean by the RCA method and then put in a quartz oven during 4 hours at 1175°C to achieve a silica thickness of 1.6 μm . Once the lower cladding is formed, organic patens are shaped using deep UV lithography at 248 nm, which offers higher precision compared to classical ‘i-line’ photolithography at 365 nm. The polymer resin is spread by spin-coating technique onto the previously oxidized silicon wafer, followed by lithography using a mask aligner

(MJB4 Mask Aligner Suss MicroTec). The mask used for lithography was designed by a software (Cadence Virtuoso) and fabricated by a company (TOPPAN PHOTOMASK Inc.). One illumination with a mercury lamp (HBO 1000W/D, OSRAM) and a dedicated filter at the desired wavelength of $\lambda = 248 \text{ nm}$ was sufficient to achieve the desired μm -scale patterns. Following lithography, the circuits were developed using tetra-methyl ammonium hydroxide (Microposit MF CD-26). A summary of the process is provided in Table 1 and the Figure 2 displays a Scanning Electron Microscope (SEM) image of the structure developed. After cleaving the wafer using a diamond tip, the photonic chip is incorporated onto the test platform.

Spin-coating (v,a,t) Softbake Deep UV exposure Post-exposure soft-bake Development Final softbake	(900 rpm, 5000rpm/s, 30s), thickness 800-850 nm, roughness $< 3 \text{ nm}$ time = 3 min, temperature = 140°C Energy = 20 mJ/cm^2 , time = 27 s time = 1 min, temperature = 120°C time = 30 s with Microposit MF CD-26 time = 12 to 24 h, temperature = 120°C
--	--

Table 1. Photolithography procedure for the photonic circuits fabrication.

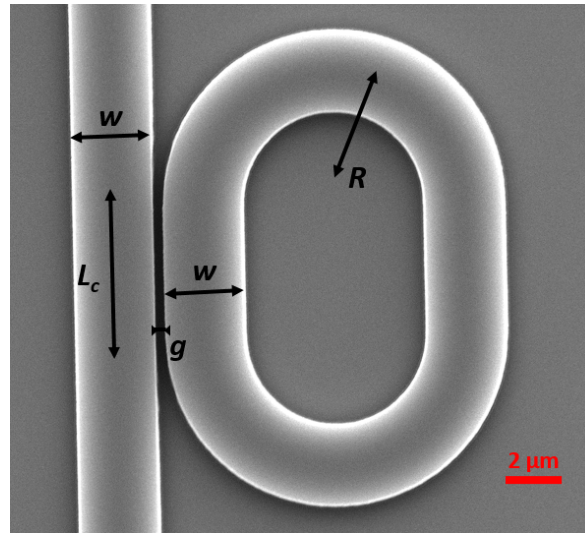


Figure 2. Scanning Electron Microscope (SEM) image of a racetrack MR coupled to a bus straight waveguide with $R = 5 \mu\text{m}$, $L_c = 5 \mu\text{m}$, $w = 5 \mu\text{m}$ and a gap of 400 nm.

2.2 Experimental set-up and measurements protocol

The resonances are excited using a broadband laser diode (Superlum SLD 331 HP3) with a central wavelength of $\lambda_0 = 795 \text{ nm}$ and a spectral width of $FWHM = 40 \text{ nm}$. The utilization of a broadband laser allows the study of multiple resonance at the same time which is necessary for extracting the FSR. A tank containing 170 μL of a water/glycerol mixture at various glycerol concentrations is placed on the surface of the photonic chip (Figure 3). Then, a solution containing silica nanoparticles (CORPUSCULAR INC. silica NPs with diameter = 600 nm, concentration = 10 mg/mL) is added using a micro-liter pipette (SATORIUS PROLINE PLUS). The resulting structure in terms of medium becomes $\text{SiO}_2/\text{UV210}/\text{Composite Medium}$. The output is connected to an Optical Analyser (OSA ANDO AQ-6315E) or a spectrometer (OCEAN OPTICS HR4000) enabling continuous acquisition of the transduced spectra throughout the entire sedimentation process via a MATLAB program. This one is also employed to extract the FSR from the data by performing a Fast Fourier Transform (FFT) on the recorded spectra by doing a Lagrangian interpolation around the peak to determine the pseudo period of the

spectra. Simultaneously, rheological measurements are conducted to compare with the optical measurements. For this purpose, a commercial rheometer (ANTON PAAR MCR 301) is utilized to measure the viscosity of various water/glycerol mixtures with different glycerol concentrations. A rheometer measures a fluid viscosity on a shear rates range which is defined as the ratio of the plate displacement velocity divided by the fluid thickness and is expressed in s^{-1} . The rheometer used in this study, with its “cone-plane” geometry,¹⁴ ensures a constant shear rate throughout the entire volume of the water-glycerol + NPs sample mixture. This is achieved because far away from the rotation axis, both the rotational speed and the mixture thickness increase and it therefore maintains an uniform shear rates across the sample.

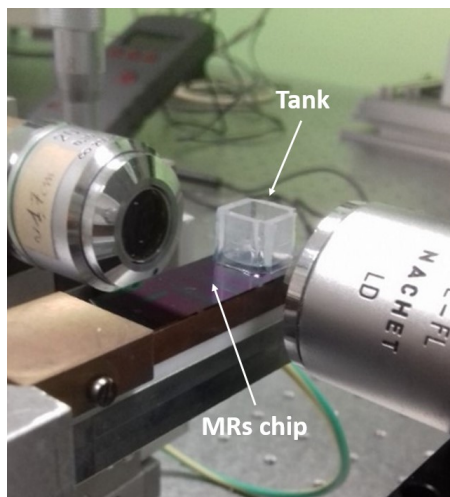


Figure 3. Photography of a tank filed by the water/glycerol mixture placed at the surface of the integrated chip during a sedimentation process.

3. RESULTS

3.1 Rheological measurements

Mechanical rheological measurements were conducted at 22°C using 3 samples of water/glycerol mixtures with the addition of a silica nanoparticle solution. The silica nanoparticles have a uniform diameter of 600 nm and the NPs solution concentration is set at $C = 10$ mg/mL. The three glycerol concentrations in the mixtures are 10%, 20% and 30%. A few milliliters of the “mixture + NPs” were required to perform the rheological measurements. Two measurements were conducted on each sample and the viscosity measurements plotted against shear rates are presented in Figure 4.a. The average viscosity values obtained are $\eta_{10\%} = 1.371$ mPa.s, $\eta_{20\%} = 1.745$ mPa.s and $\eta_{30\%} = 2.946$ mPa.s. Figure 4.b depicts the plot of the average viscosity for each sample as a function of the glycerol concentration. It is evident that the viscosity increases with higher glycerol concentration and this relationship exhibits a nonlinear behavior.

3.2 Optical resonant measurements

In a previous study, the sedimentation of silica NPs in pure water has been extensively investigated, considering various diameters and concentrations.¹⁵ The behavior of NPs during sedimentation has been described using theoretical models based on the Stokes equation, and a strong correlation between surface resonant measurements and sedimentation rates has been established. In this current work, we extend the investigation of NPs sedimentation to approach a viscosity measurement by studying four different mixtures with glycerol concentrations set at 0%, 10%, 20%, and 30%. Spectra were recorded continuously throughout the entire sedimentation process, and Fast Fourier Transform (FFT) analysis was performed to extract directly the Free Spectral Range (FSR) for each sample. For this purpose, a 5 μ L solution containing NPs was added to a water/glycerol mixture in a tank positioned on the surface of the integrated chip. The FSR evolution was recorded during the entire

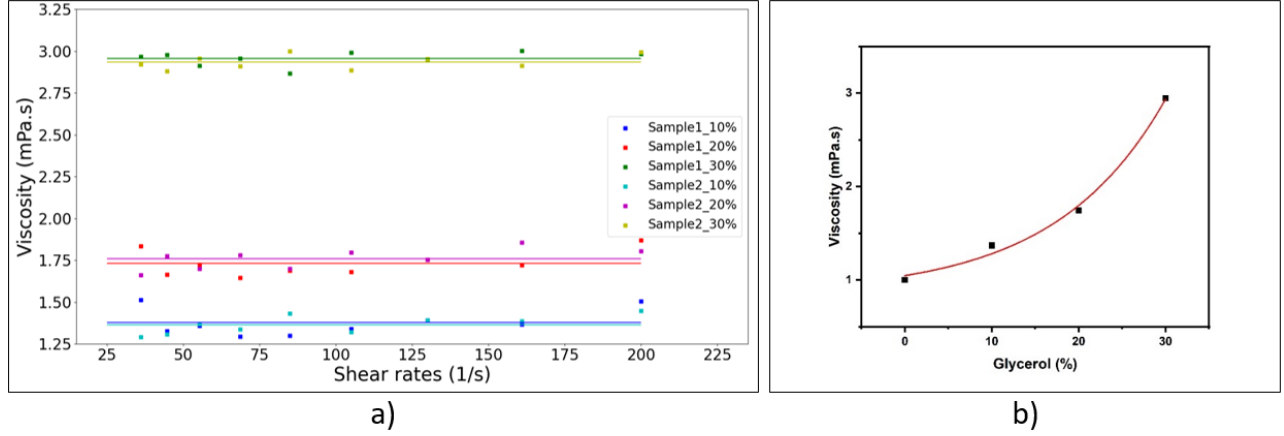


Figure 4. a) Viscosity versus the shear rates for 3 mixture "water/glycerol + silica NPs" at 3 glycerol concentration (10, 20, 30 %) with twice measurements for each sample. It gives 3 averages viscosity : $\eta_{10\%} = 1.371 \text{ mPa.s}$, $\eta_{20\%} = 1.745 \text{ mPa.s}$ and $\eta_{30\%} = 2.946 \text{ mPa.s}$. b) Average viscosity of each sample as a function of the glycerol concentration where the non-linearity clearly appears. The fitting curve is set as $y = 0.85 + 0.19.exp(0.079x)$.

sedimentation process and plotted in real time as a function of time for the four concentrations in Figure 5. The FSR increases over time for all glycerol concentrations. It is indeed multiplied by a factor of 1.3 – 1.4 between the beginning and the end of the sedimentation process. The silica nanoparticles can be visualized as a cloud-like matter that descends until it reaches the surface of the chip. The upper cladding is perceived by the light as a composite effective medium, wherein the silica fraction within the host medium changes as the cloud is migrating plus sedimenting. Hence, as the interface change from UV210/Mixture to UV210/Mixture+NPs and due to the increased density of the NPs cloud resulting from compression, the effective index of the overall structure decreases. Since the refractive index of silica is higher than the water/glycerol one, the light becomes less confined. In other words, the refraction index difference between the core and the upper cladding becomes less important. With the light being dispersed more outside the core of the structure, the effective index of the global structure becomes smaller. Given that $FSR = \frac{\lambda_0^2}{P.n_{eff}^2}$, the FSR increases as the NPs cloud is sedimenting and undergoing compression, leading to an increased density.

The stabilization of the FSR indicates the completion of sedimentation, marking the time when the NPs cloud reaches the surface. The corresponding stabilization times are $t_{sed,0\%} = 143 \text{ min}$, $t_{sed,10\%} = 164 \text{ min}$, $t_{sed,20\%} = 190 \text{ min}$ and $t_{sed,30\%} = 230 \text{ min}$. It is expected that the sedimentation process takes longer for higher glycerol concentration. Figure 6 presents the experimental contact times determined from FSR evolution, along with the theoretical predictions obtained using the Stokes model. Applying the second law of Newton to an isolated silica nanoparticle leads to the sedimentation velocity $v_{Stokes} = \frac{2}{9} \frac{gR^2(\rho_{NP} - \rho_{mixture})}{\rho_{mixture}}$ where $\rho_{mixture} = x\rho_{glycerol} + (1-x)\rho_{water}$ according to the Végard law with x the glycerol fraction. By substituting the values $R = 300 \text{ nm}$, $\rho_{NP} = 2650 \text{ kg/m}^3$ and $\rho_{glycerol} = 1260 \text{ kg/m}^3$, the theoretical contact time is calculated using $v_{Stokes} = \frac{h}{t}$ with h the mixture height set as $h = 3 \text{ mm}$. As the glycerol concentration increases, the disparity between the experimental and theoretical results becomes more pronounced. The Stokes model does not consider the interactions between nanoparticles, which becomes significant when their number is substantial and particularly important for low viscosity system. Another approach more precise involves measuring the effective viscosity $\eta_{eff} = \eta_{mixture}(1 + 2.5\phi)$ depending on the volume fraction of nanoparticles. This approach leads to another average velocity expressed as $\langle v \rangle = v_{Stokes}f(\phi) = v_{Stokes}(1 - \phi)^n$, where n is a numerical factor.^{15,16} However, the classical Stokes model is sufficient for direct comparison between experimental and theoretical results.

FSR oscillations can be observed on each graph except for the more viscous one. The addition of the NPs solution alters the surface tension of the mixture and the concentration of NPs is not uniform throughout the entire volume, resulting in a concentration gradient. Those surface tension and concentration gradient induce

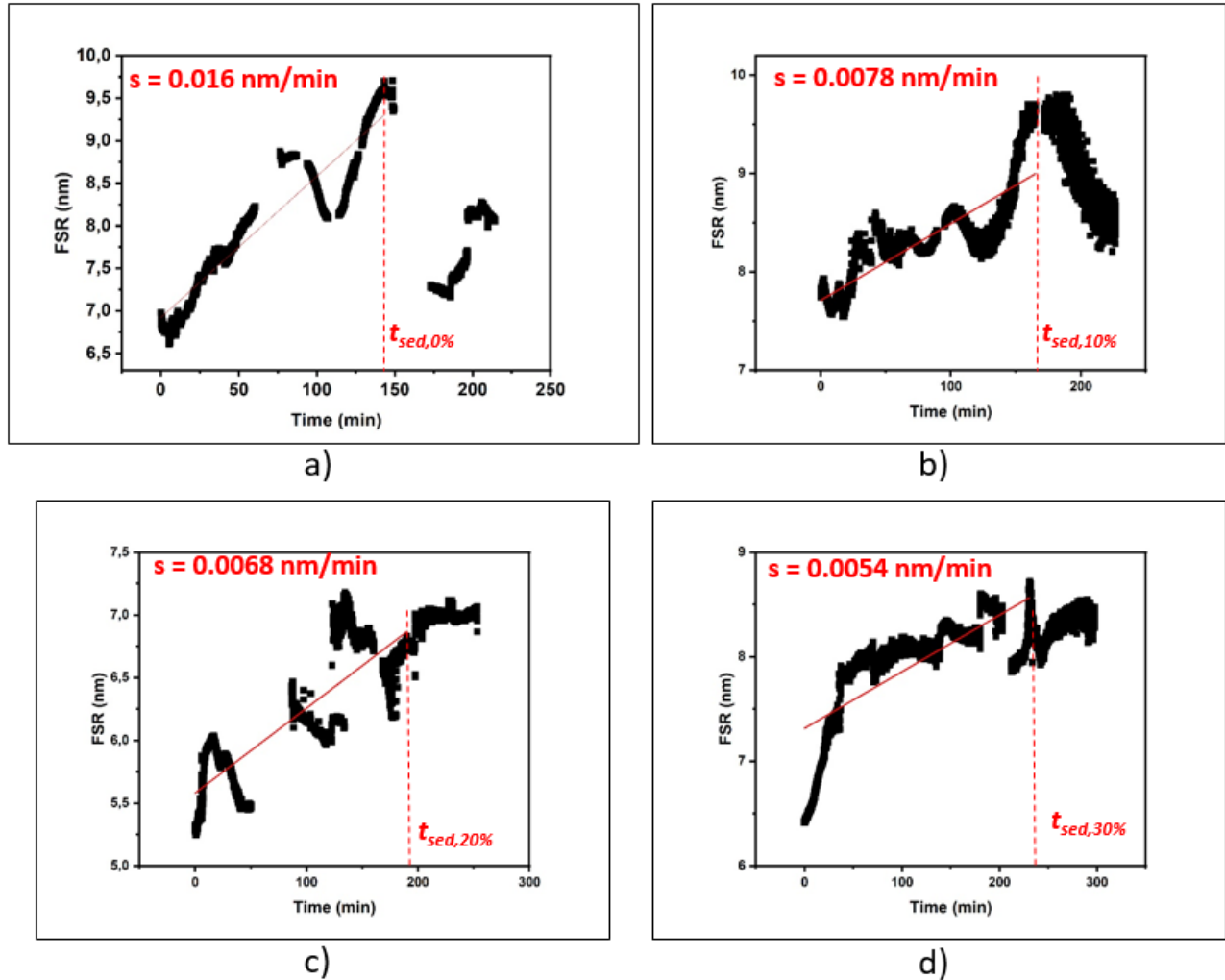


Figure 5. FSR evolution as a function of time during a sedimentation process of silica NPs in a water/glycerol mixture at different concentration : a) 0% b) 10% c) 20% and d) 30%. In red, the FSR slope s variation corresponding to the sedimentating plus migrating phase.

vortices and movements, known as the Marangoni effect.^{17,18} In viscous liquids, this effect is less pronounced, leading to less significant or even invisible oscillations (as observed in the case of a glycerol concentration equals to 30%). Moreover, it is noticeable that for glycerol concentrations of 0% and 10%, the FSR initially increases until reaching a maximum value, then decreases before stabilizing. In contrast, for viscous mixtures, the FSR stabilizes immediately after the sedimentation process. The second phase of stabilization, accompanied by the compression and densification of the silica cloud, is attributed to a pinning effect.¹⁵ This effect arises due to the non-infinite dimension of the tank placed above the chip, resulting in curvature at the interface between the mixture and the air. The evaporation is more pronounced in the center of the tank compared to the edges, resulting in an increased curvature. This increase will “sweep” NPs at the surface of the chip, leading to their re-arrangement and a stabilization that affect the FSR evolution. It is worth noting that this phenomenon is more prominent for fluids with medium viscosity closer to that of water.

The slope s of the $FSR(t)$ variation can be obtained from the spectra and the plot of the slope s as a function of the glycerol concentration is shown in Figure 7. By drawing an analogy with the plot of viscosity measured by the mechanical rheometer (Figure 4.b), it is possible to establish a mathematical relationship between the

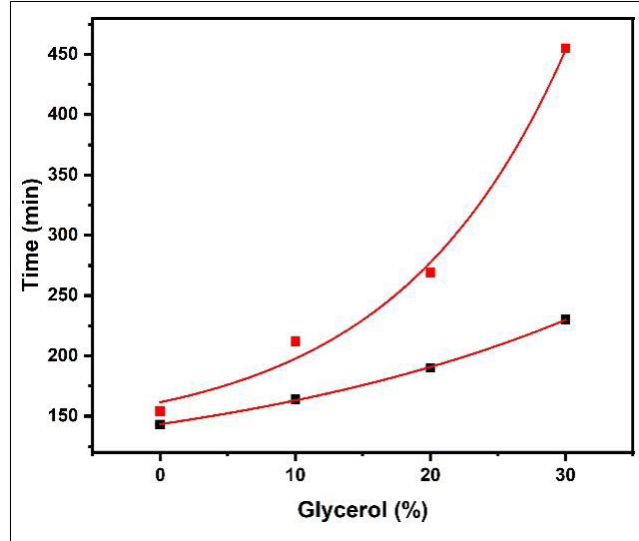


Figure 6. Experimental contact time measured by optical resonant signal in black (slope inversion of the FSR evolution) and theoretical contact time ($t = \frac{h}{v_{Stokes}}$) calculated with the simple Stokes model in red as a function of the glycerol concentration. The fitting curves are set as $y_{exp} = 93.37 + 48.02exp(0.034x)$ and $y_{th} = 131.66 + 29.87exp(0.079x)$.

viscosity and the slope of the FSR(t). By measuring the resonant signal of a mixture during the sedimentation process and calculating its FSR(t) evolution, the viscosity of the mixture can be determined.

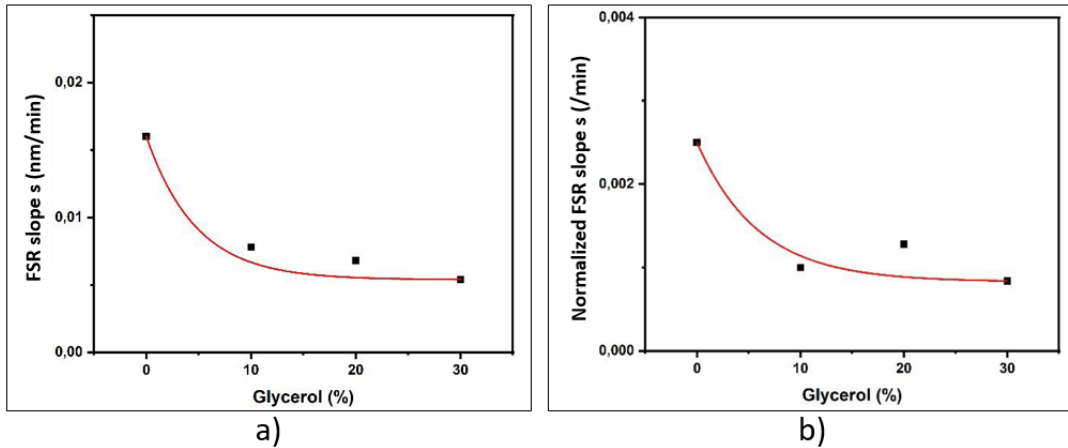


Figure 7. a) Experimental FSR slope s during silica NPs sedimentation process in water/glycerol mixture with four glycerol concentration : 0%, 10%, 20% and 30%. The fitting curve is set as $y = 0.0053 + 0.01exp(-\frac{x}{4.75})$ b) Normalized FSR slope s as a function of the glycerol concentration with the fitting curve set as $y = 8.29.10^{-4} + 0.017exp(-\frac{x}{5.5957})$.

4. CONCLUSION

This study presents a novel approach to measuring viscosity using an optoelectronic resonant device. A nanotechnology process was employed to fabricate resonant structures consisting of racetrack micro-resonators coupled to taper waveguides. Photolithography at 248 nm was utilized to pattern the UV210 polymer with micrometer-scale features and a 400 nm gap. The resulting photonic device was integrated into an optical measurement setup to monitor in real time the evolution of the resonant signal during a sedimentation process. The sedimentation process causes changes in the effective index of the overall structure, leading to variations in the FSR(t) evolution. A direct correlation can be observed between the normalized slope s of the FSR evolution (Figure 7.b) and the inversed contact time (Figure 6) : $s(\text{min}^{-1}) \propto \frac{1}{\text{Time}}$. The obtained optical measurements were found to agree well with mechanical rheological measurements, enabling the determination of viscosity using such optoelectronic resonant sensor. Such device is mostly designed as a quasi-surface configuration rather than a bulk configuration, making it well-suited for applications involving colloidal systems or dark substances.

Acknowledgments : The authors would like to thank the “Fondation d’Entreprise Grand Ouest” (BPGO) plus the “Fondation Rennes 1” for the financial support and the SATT Ouest Valorisation for supported the project “Solution 3M”.

The authors also thank the NanoRennes platform for the DUV process (<https://www.ietr.fr/en/nr-nanorennnes-platform>). This work was carried out in parallel with a “cordée de la réussite” program at “Université de Rennes” : <https://www.univ-rennes.fr/actualites/quand-les-eleves-cherchent-avec-les-chercheurs>.

REFERENCES

- [1] Yu, M., Le Floch-Fouéré, C., Pauchard, L., Boissel, F., Fu, N., Chen, X. D., Saint-Jalmes, A., Jeantet, R., and Lanotte, L., “Skin layer stratification in drying droplets of dairy colloids,” *Colloids and Surfaces A: Physicochemical and Engineering Aspects* **620**, 126560 (2021).
- [2] Guibet, J.-C., “Caractéristiques des produits pétroliers,” *Techniques de l’ingénieur Caractérisation et propriétés de la matière* (ref. article : k325) (1997).
- [3] Garnier, L., Lhermite, H., Labouret, T., Saint-Jalmes, A., Cormerais, H., Vié, V., and Bêche, B., “On the dynamic monitoring of the variations in blood viscosity by resonant optical signal,” *Proceedings of SPIE, the International Society for Optical Engineering*, **12139**, 89–96 (2022).
- [4] Qian, G., Zhang, T., Zhang, L.-J., Tang, J., Zhang, X.-Y., Lu, Y., and Wan, F.-H., “Demonstrations of centimeter-scale polymer resonator for resonant integrated optical gyroscope,” *Sensors and Actuators A: Physical* **237**, 29–34 (2016).
- [5] Rabiei, P., Steier, W. H., Zhang, C., and Dalton, L. R., “Polymer micro-ring filters and modulators,” *Journal of lightwave technology* **20**(11), 1968 (2002).
- [6] Chao, C.-Y., Fung, W., and Guo, L. J., “Polymer microring resonators for biochemical sensing applications,” *IEEE journal of selected topics in quantum electronics* **12**(1), 134–142 (2006).
- [7] Castro-Beltrán, R., Garnier, L., Saint-Jalmes, A., Lhermite, H., Cormerais, H., Fameau, A.-L., Gicquel, E., and Bêche, B., “Microphotronics for monitoring the supramolecular thermoresponsive behavior of fatty acid surfactant solutions,” *Optics Communications* **468**, 125773 (2020).
- [8] Garnier, L., Lhermite, H., Vié, V., Pin, O., Liddell, Q., Cormerais, H., Gaviot, E., and Bêche, B., “Monitoring the evaporation of a sessile water droplet by means of integrated photonic resonator,” *Journal of Physics D: Applied Physics* **53**(12), 125107 (2020).
- [9] Rabus, D. G., [*Integrated ring resonators*], Springer (2007).
- [10] Tamir, T., Griffel, G., and Bertoni, H. L., [*Guided-wave optoelectronics: device characterization, analysis, and design*], Springer Science & Business Media (2013).
- [11] Castro-Beltrán, R., Huby, N., Vié, V., Lhermite, H., Camberlein, L., Gaviot, E., and Bêche, B., “A laterally coupled uv210 polymer racetrack micro-resonator for thermal tunability and glucose sensing capability,” *Advanced Device Materials* **1**(3), 80–87 (2015).
- [12] Mahé, F., Garnier, L., and Bêche, B., “Analysis of giant waveguide tapers with funnel geometry: multi-mode interference regime to single mode,” *Proceedings of SPIE, the International Society for Optical Engineering*, **11775**, 167–172 (2021).

- [13] Castro-Beltran, R., Huby, N., Loas, G., Lhermite, H., Pluchon, D., and Bêche, B., “Improvement of efficient coupling and optical resonances by using taper-waveguides coupled to cascade of uv210 polymer micro-resonators,” *Journal of Micromechanics and Microengineering* **24**(12), 125006 (2014).
- [14] Dupuis, D. and Ponton, A., “Mesure de la viscosité viscosimètres et rhéomètres,” *Techniques de l'ingénieur Mesures physiques* (ref. article : r2351) (2021).
- [15] Garnier, L., Gastebois, J., Lhermite, H., Vié, V., Saint-Jalmes, A., Cormerais, H., Gaviot, E., and Bêche, B., “On the detection of nanoparticle cloud migration by a resonant photonic surface signal towards sedimentation velocity measurements,” *Results in Optics* **12**, 100430 (2023).
- [16] Richardson, J. T., “Sedimentation and fluidization: Part i,” *Trans. Inst. Chem. Engrs.* **32**, 35–52 (1954).
- [17] Marangoni, C., “Sul principio della viscosità superficiale dei liquidi stabilito dal sig. j. plateau,” *Il Nuovo Cimento (1869-1876)* **5**, 239–273 (1871).
- [18] Le Roux, S., *Effet Marangoni aux interfaces fluides*, theses, Université de Rennes (July 2015).